SUPPLEMENTARY MATERIAL

Mutational analysis of a conserved glutamate reveals unique mechanistic and structural features of the phosphatase PRL-3

Birgit Hoeger[1], Pablo Rios[1,2], Anna Berteotti[1], Bernhard Hoermann[1,2,3], Guangyou Duan[1] and Maja Köhn[1,2]*

[1]European Molecular Biology Laboratory, Genome Biology Unit, Meyerhofstrasse 1, 69117 Heidelberg, Germany
[2]Faculty of Biology and Centre for Biological Signalling Studies (BIOSS), University of Freiburg, Schänzlestr 18, 79104, Freiburg, Germany
[3]University of Heidelberg, Germany

*Corresponding author: Maja Köhn, Email: maja.koehn@bioss.uni-freiburg.de

INDEX

1. Supplementary Figures

Figure S1:

Kinetic raw data of DiFMUP dephosphorylation (corresponding to Table 1a).

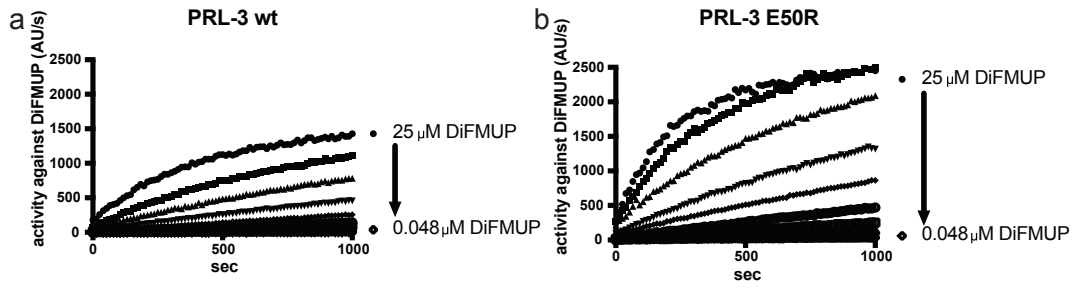

Figure S2:

CD spectroscopic data of various PRL-3 variants, showing no significant change of protein fold upon introduction of the respective mutation(s).

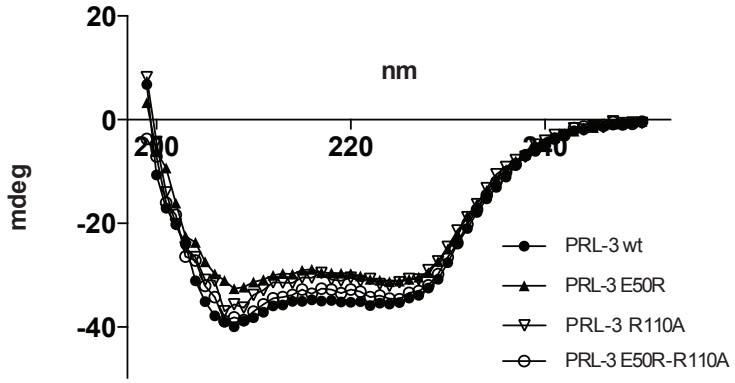

Figure S3:

a) Isothermal titration calorimetry confirms the lacking interaction of PRL-3 variant E50R-R110A with DiFMUP, as shown by the respective catalytically inactive C104S-variant (left, E50R-R110A-C104S). The raw data confirm binding interaction of variants C104S (middle) and E50R-C104S (right) with DiFMUP. Due to the generally low enthalpy change, K_d values could not be determined quantitatively. b) CD data of the respective variants. Gray data points could not be compared to the rest of the data due to signal overload on the detector. Variant C104S was newly cloned and purified for this experiment and showed wild-type-like protein fold characteristics, in contrast to previously published data[14]. For PCR, the following C104S-specific primer pair was used: 5' ctgtgcactccgtggcggg 3' and 5' cccgccacggagtgcacag 3'.

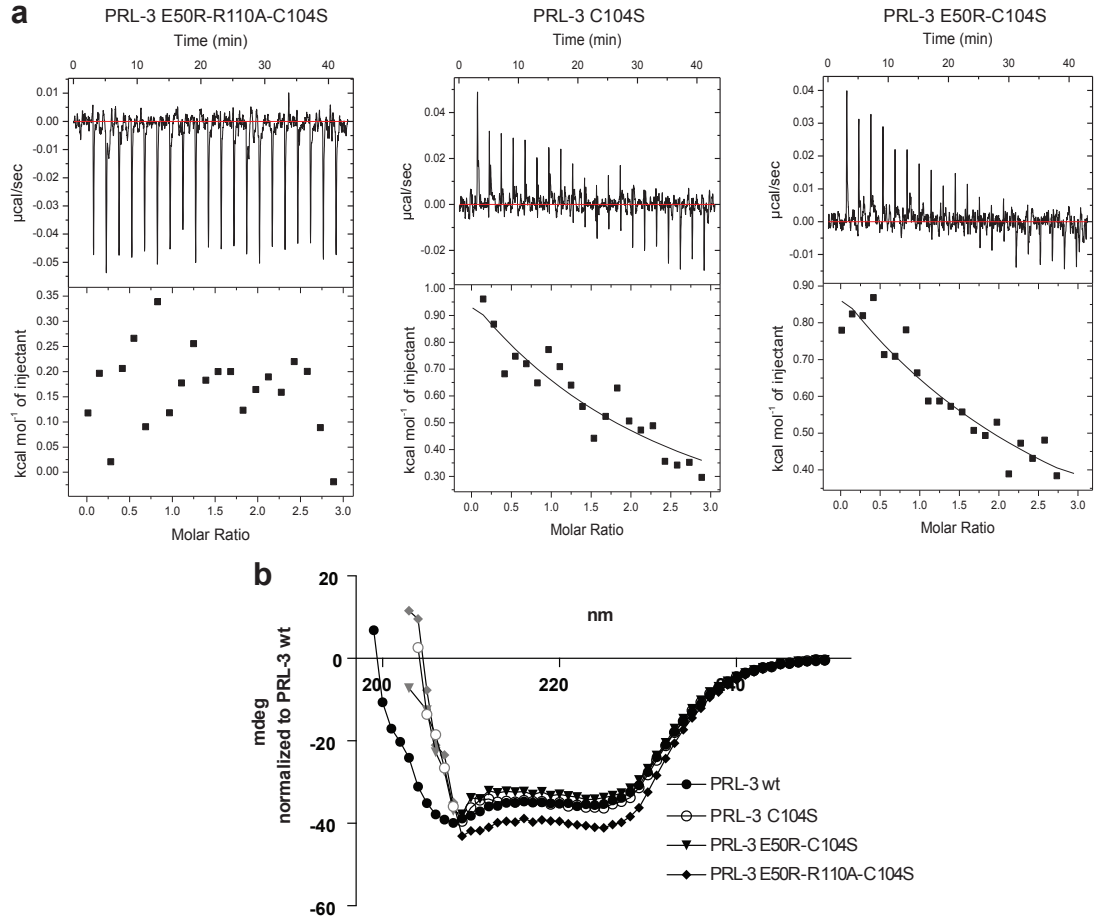

Figure S4:

Enzymatic activities of PRL-3 wt and C49A, showing the inability of C49A to get reduced after full oxidation (a). b) Corresponding non-reducing SDS gel images, showing the inability of variant C49A to form a disulfide bridge with the catalytic cysteine residue in oxidative environment. Oxidized forms correspond to lower band shifts due to disulfide bond formation. c-d) PRL-3 wt and E50R show similar redox profiles and reversible oxidation. Enzymatic activity followed similar trends and plateau levels in both cases, regarding oxidation (inactivation) after full reduction with DTT (c) or reduction (re-activation) after full oxidation with hydrogen peroxide (d). Experiments were performed as described in the Supplementary Methods section.

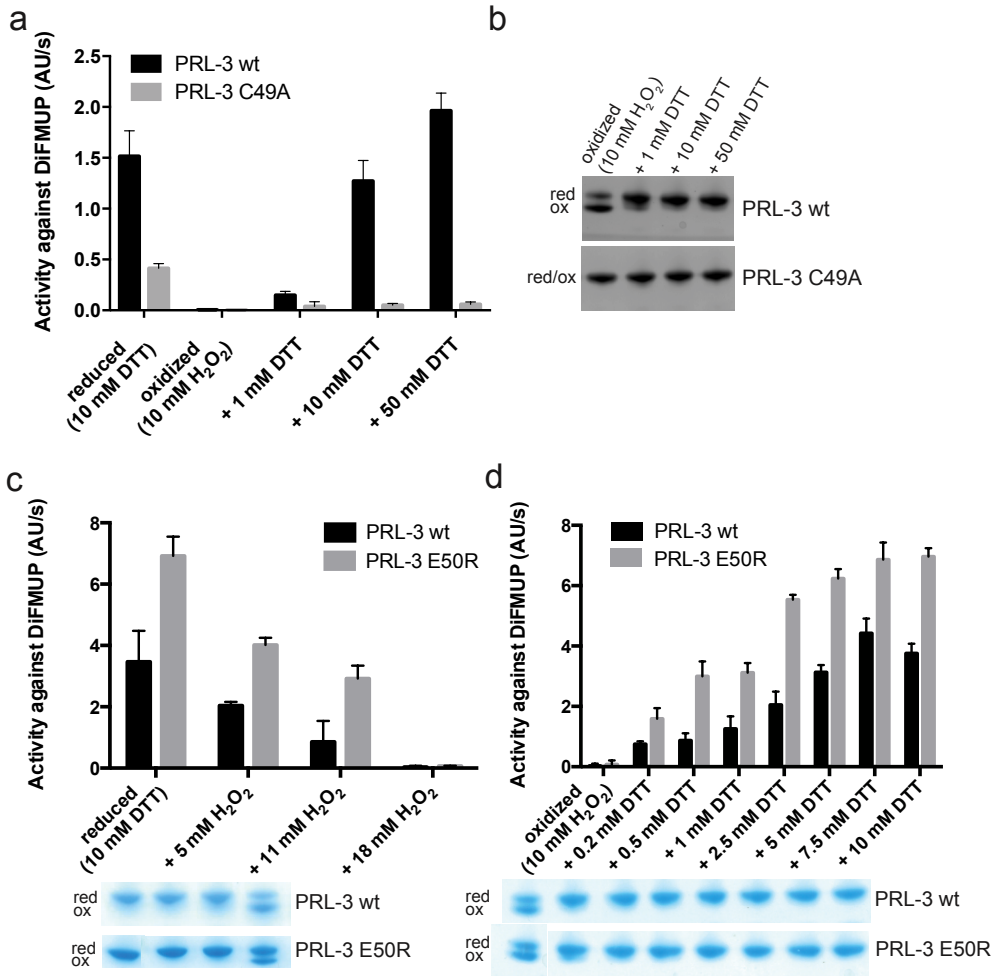

Figure S5

Analysis of the surface potential of PRL-3 and PRL-1 when introducing the E50R mutation. The electrostatic potential was calculated trough http://nbcr-222.ucsd.edu/pdb2pqr_2.1.1/ and plotted on the surface of the proteins with pymol using the protonation state of the proteins at pH 7.0. pdb entry numbers are indicated on the right next to the structures.

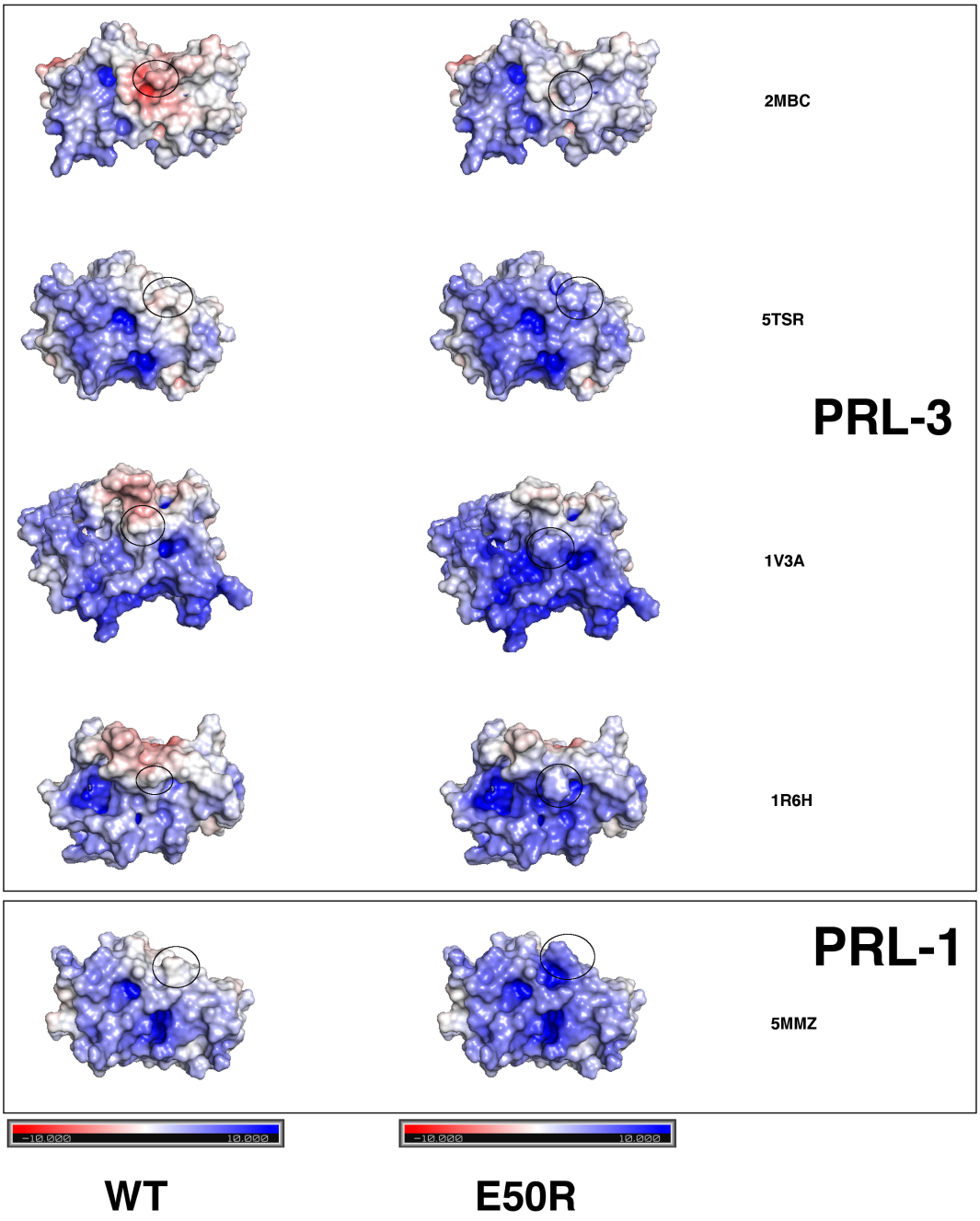

Figure S6:

Migration and adhesion analysis on various supports. a-d) HEK293 PRL-3 and E50R cells migrate like control cells on laminin, collagen-IV, gelatin and collagen-I substratum; e-h) HEK293 PRL-3 and E50R cells adhere to laminin, collagen-IV and gelatin like control cells. The effect on collagen-I was statistically marginally significant, but not of biological relevance. Cells were seeded on the respective support and analyzed by microscopy for percentage of adhering cells or for speed of migration (where applicable). Results are shown as mean ± SD. Statistics, compared to control: * p 0.0282; ** p 0.0099; ns – not significant.

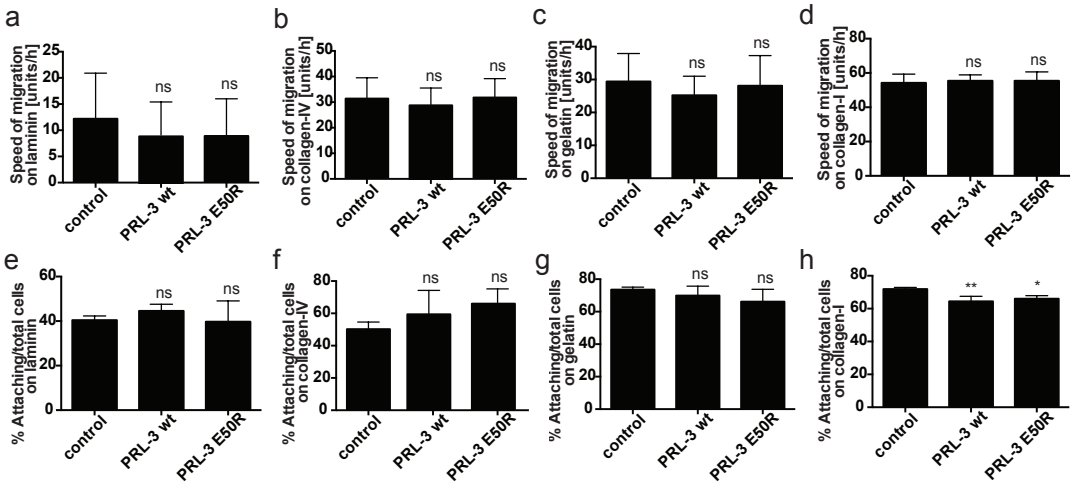

Figure S7:

HEK293 PRL-3 (E50R) cells show unpredictable migration abilities on various types of uncoated plastic support. While PRL-3 but not E50R cells showed enhanced phenotype on Ibidi dishes (a), E50R had decreased migration abilities on Nunclon plates (b). No effect was seen for any cell line on Mattek plastic support (c). The respective providers informed that different treatments of plastic for tissue culture were applied (the exact treatments are confidential). Results are shown as mean ± SD. Statistics, compared to control or where indicated: **** p 0.0001; ns – not significant.

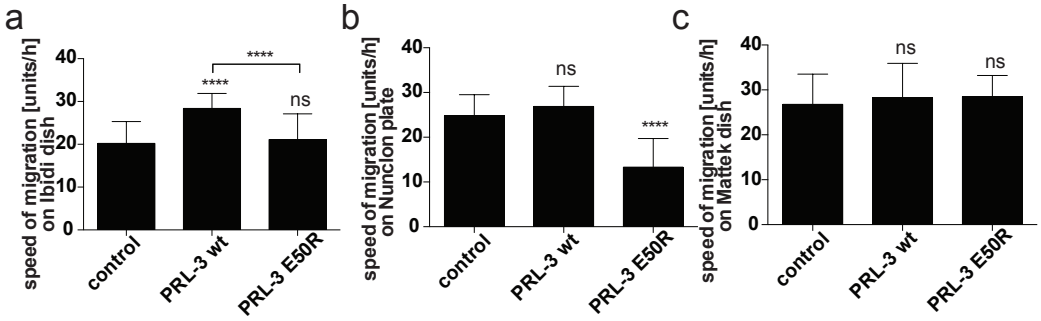

Figure S8:

HEK293 PRL-1 cells migrate slower than the PRL-3-expressing counterpart, but faster than the control cell line on uncoated plastic support from Ibidi. Results are shown as mean ± SD. Statistics, compared to control or where indicated: **** p 0.0001.

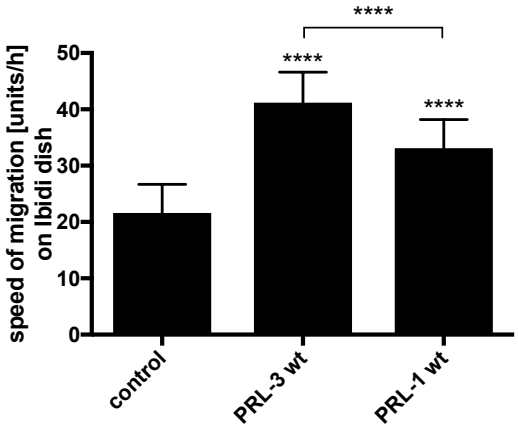

Figure S9:

Original widefield microscopy images for HEK293 cell adhesion on fibronectin. 20 minutes after seeding, considerably more PRL-3 wt cells had attached compared to control cells, as indicated by the increased percentage of flat cells showing visible protrusions, in contrast to the round unattached cells. Almost all E50R cells had already attached at this time point.

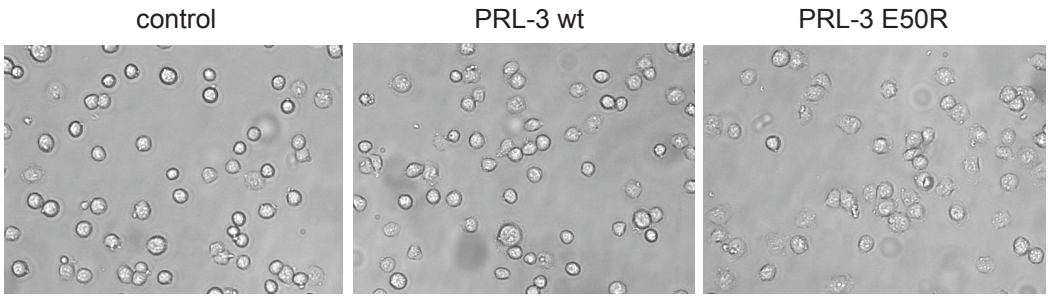

2. Supplementary Methods

Isothermal titration calorimetry

To test for binding interactions between DiMFUP and PRL-3 variants, isothermal titration calorimetry (ITC) was used. For cloning of the respective catalytically inactive variants C104S, E50R-C104S and E50R-R110A-C104S, see the respective experimental section. Proteins were dialyzed into ITC buffer (20 mM Tris-HCl, pH 7.5, 150 mM NaCl, 0.01% triton-X 100, 1% DMSO). After dialysis, the very same buffer was used to solubilize DiFMUP. ITC experiments were performed at 25 °C using a MicroCal iTC200 micro calorimeter (GE Healthcare). Titrations were performed with 50 µM protein in the cell chamber and 750 µM ligand concentration for the titration syringe. ITC data were corrected for the dilution heat and analyzed with MicroCal Origin^{TM} software.

Redox activity study

Redox stability of PRL-3 wt and variants was compared at varying concentrations of oxidizing and reducing agent. Proteins were dialyzed into 20 mM Tris-HCl pH 7.5, 150 mM NaCl and set to a concentration of 0.55 mg mL-1. For the oxidation experiments, proteins were fully reduced with 10 mM DTT and incubated for 30 min at 4 °C. Proteins were then re-oxidized by addition of varying concentrations of H_2O_2, as indicated, and incubation at room temperature for 30 min. 10 U catalase (Sigma) was added to consume residual H_2O_2 and the reaction was kept at room temperature for 3 min. Samples were then split for SDS polyacrylamide protein gel electrophoresis and phosphatase activity assays. Samples for protein gels were prepared in non-reducing sample buffer (2x buffer: 125 mM Tris-HCl pH 6.8, 20 % (v/v) glycerol, 4 % (w/v) SDS and 0.05 % (w/v) bromophenol blue), boiled at 95 °C for 7 min and loaded with 1.1 µg protein per well. DiFMUP activity assays were performed as described above, except that DTT was omitted from the assay buffer. Enzymes were monitored at 150 nM concentration. DiFMUP was used at the respective Km value (21 µM for wt PRL-3, 22 µM for PRL-3 E50R, 33 µM for PRL-3 C49A). For reduction experiments after full oxidation, proteins were first oxidized with 10 mM H_2O_2 for 30 min, treated with 10 U catalase and re-reduced with the indicated concentrations of DTT. Samples were then split for protein gels and activity assays, as

before. For site-directed mutagenesis of the C49A variant, the following primer pair was used: 5’ gtgcgtgtggctgaagtg accta 3’ and 5’ taggtcacttcagccacacgcac 3’.

Migration and adhesion studies on various supports

Adhesion and migration studies were performed according to the main methods section. Collagen-I and collagen, IV were monitored 30 min after seeding, laminin 2h and gelatin 4.5 h after seeding. Independent experiments were performed at least in triplicates (collagen-I) or duplicates (other coatings). Migration experiments on various kinds of matrix or plastic support were monitored 4h and 7h after initiation of migration.